1987-02-15

Response of the upper ocean to a large summertime injection of smoke in the atmosphere

Mettlach, T.R.; Haney, R.L.; Garwood R.W. Jr.; Ghan, S.J.

American Geophysical Union

Journal Name: J. Geophys. Res.; (United States); Journal Volume: 92:C2
http://hdl.handle.net/10945/60959

JOURNAL OF GEOPHYSICAL RESEARCH, VOL. 92, NO. C2, PAGES 1967–1974, FEBRUARY 15, 1987

The Response of the Upper Ocean to a Large Summertime Injection of Smoke in the Atmosphere

THEODORE R. METTLACH AND ROBERT L. HANEY

Department of Meteorology, Naval Postgraduate School, Monterey, California

ROLAND W. GARWOOD, JR.

Department of Oceanography, Naval Postgraduate School, Monterey, California

STEVEN J. GHAN

Lawrence Livermore National Laboratory, University of California, Livermore

A one-dimensional oceanic planetary boundary layer model is used to investigate the response of the upper ocean to the atmospheric conditions which are predicted to develop following a hypothetical nuclear exchange. The ocean model is driven by the surface heat and momentum fluxes predicted by an atmospheric general circulation model following a summertime injection of 1.5×10^{14} g of smoke from postwar fires over Europe, Asia, and North America. Although the specific response of the upper ocean is highly dependent on the geographic location, the mid-latitude summertime mixed layer typically cools 3° to 5°C and deepens 25 m during the first 30 days following the smoke injection. Moreover, a large fraction of this response is found to take place during a short 2- to 3-day period of very intense winds and falling air temperatures, which occurs during the first week or two after the smoke injection.

INTRODUCTION

In the past 5 years much attention has been given to the potential climatic consequences of a major nuclear exchange between the superpowers. One result of this attention has been the development of the "nuclear winter" hypothesis that tremendously large amounts of smoke injected into the atmosphere from the fires from hundreds of nuclear detonations during a major nuclear exchange would block enough sunlight that the interiors of the northern hemisphere's continents would cool ~10°–30°C for periods of the order of a month. This hypothesis has developed as a result of the initial studies by *Crutzen and Birks* [1982], who calculated the amount of smoke that is produced by a large number of massive fires, and by *Turco et al.* [1983], who investigated the one-dimensional radiative-convective response of the atmosphere to certain smoke aerosol injection scenarios. The major conclusions of Turco et al. have been substantiated and further refined by two-dimensional [*MacCracken*, 1983] and three-dimensional [*Aleksandrov and Stenchikov*, 1983; *Covey et al.*, 1984; *Cess et al.*, 1985] atmospheric simulations with fixed distributions of smoke and by two-dimensional [*Haberle et al.*, 1985] and three-dimensional [*MacCracken and Walton*, 1984; *Stenchikov*, 1985; *Malone et al.*, 1986; *Thompson*, 1985] atmospheric simulations in which smoke is transported and removed by the evolving atmospheric circulation. In the three-dimensional simulations, both the magnitude and the geographical distribution of surface air temperature reductions are modified by the vast (assumed infinite in most simulations) heat capacity of the underlying oceans.

Since the oceans have been found to play such an important role in the atmospheric simulations of nuclear winter, it is surprising that with the exception of the Soviet work, no serious attempt has yet been made to investigate the ocean's response to such nuclear war scenarios. *Robock* [1984] examined the nuclear winter hypothesis using a seasonal energy balance climate model based on that of *Sellers* [1973] coupled to an ocean model with a constant (in time) mixed layer depth. In response to plausible nuclear winter scenarios, the coupled model predicted sea surface temperature (SST) decreases ~11°C in 100 days in mid-latitudes. In the present study we use a physically realistic one-dimensional ocean planetary boundary layer model to investigate the short-term consequences in the ocean of a three-dimensional atmospheric general circulation model's response to smoke generated by a full-scale nuclear exchange. We consider only a northern hemisphere summer case (July) because previous atmospheric model simulations [*Covey et al.*, 1984] indicate that the atmosphere's response to a nuclear exchange is much stronger in summer, when more solar radiation is available for absorption by the smoke, than in winter.

We have focused our study on the short-term response of the ocean because of the large uncertainties associated with estimating the potential response of the atmosphere to a full-scale nuclear exchange. These uncertainties fall into two major categories [*Berger*, 1986]. The first concerns the amount, distribution, and physical properties (size, shape, and blackness) of the smoke produced during and immediately after a nuclear exchange. These uncertainties are due to our limited knowledge of the specific details of the nuclear exchange, the availability of combustible material, the thermodynamics and chemistry of large fires, and the properties of particulate matter in the smoke plumes. The second category concerns the ensuing effect of the smoke layer on the atmosphere and the effect of the atmosphere in dispersing or removing the smoke as well as changing the optical properties of smoke particles by aggregation or chemical reactions. As a result, reliable quantitative estimates of the atmospheric response to a nuclear exchange are probably limited to less than 1 month. For such short time scales and for the rather strong atmo-

Paper number 6C0627.
0148-0227/87/006C-0627$02.00

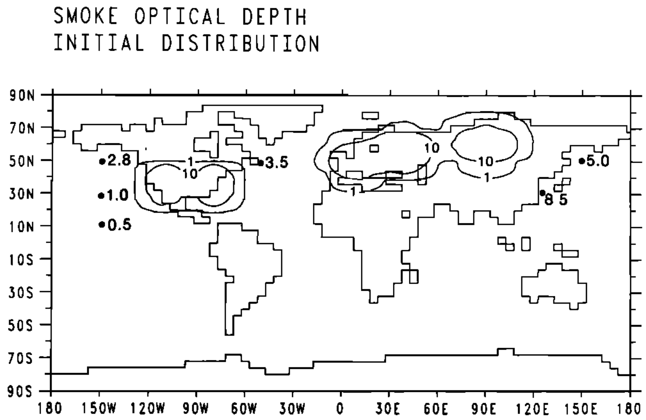

Fig. 1. The initial distribution of smoke extinction optical depth used in the atmospheric nuclear winter simulation [from *Ghan et al.*, 1985]. Dots show the locations of the ocean numerical experiments, and the number beside each dot gives the differences in SST (in degrees Celsius) after 30 days between the control and nuclear winter experiments. At all locations the SST was lower after the nuclear winter experiment.

spheric forcing that is expected, the response of the upper ocean clearly will be dominated by the local, i.e., the one-dimensional, forced response.

The Model and the Numerical Experiments

In this study we use the one-dimensional ocean planetary boundary layer model of *Garwood* [1977]. The model uses the turbulent kinetic energy budget to describe the production, dissipation, and buoyant damping of turbulent kinetic energy in the upper ocean. Separate equations for the vertical and horizontal components of turbulent kinetic energy are used, and closure is achieved by parameterizing the second- and third-order terms in the turbulent kinetic energy equations. While the Garwood model has a number of unique features which make it somewhat different from other bulk or profile models of the upper ocean, other modern mixed layer models are expected to produce qualitatively similar results [*Martin*, 1985].

Two types of numerical experiments, "control" and "nuclear winter," respectively, were carried out at six different locations in the North Atlantic and North Pacific oceans. In the control experiments, the ocean model was driven by the local wind stress and heat fluxes at the sea surface taken from a "normal" or "typical" atmospheric general circulation model simulation of the "perpetual" month of July. In the nuclear winter experiments, the surface heat fluxes and surface stresses were taken from an otherwise identical atmospheric model simulation except that a total of 1.5×10^{14} g of smoke was injected into the air over Europe, Asia, and North America. These atmospheric simulations, which made use of the Oregon State University two-level tropospheric general circulation model [*Schlesinger and Gates*, 1980; *Ghan et al.*, 1982], have been described in some detail by S. J. Ghan et al. (The climatic response to large atmospheric smoke injections: Sensitivity studies with a tropospheric general circulation model, submitted to *Journal of Geophysical Research*, 1986). In both atmospheric simulations, control and nuclear winter, the sea surface temperatures were prescribed to be July climatological values. For these studies, the atmospheric model was modified by the incorporation of a delta-Eddington formulation for solar radiation [*Cess et al.*, 1985], and in the nuclear winter simulation it was coupled to a Lagrangian trace species transport model known as GRANTOUR (J. J. Walton et al., A global-scale Lagrangian trace species transport model, sunmitted to *Journal of Geophysical Research*, 1986). By means of GRANTOUR, smoke particles, which were initially distributed uniformly with height, were subjected to dry deposition and coagulation as well as precipitation scavenging and large-scale advective transport. The particular nuclear winter experiment considered here assumes an injection of 1.5×10^{14} g of smoke with a refractive index of $m = 1.75 - 0.3i$ and a lognormal size distribution with a number mode radius of 0.1 μm and a standard deviation of 2.0. Figure 1 shows the initial distribution of the smoke as represented by the extinction optical depth [*Turco et al.*, 1983]. Values greater than 50 are found over both continents. By the end of the 30-day simulation, the smoke concentration becomes relatively uniform over the northern hemisphere, with values of optical depth in the range from 0.5 to 2.0 (S. J. Ghan et al., The climatic response to large atmospheric smoke injections: Sensitivity studies with a tropospheric general circulation model, submitted to *Journal of Geophysical Research*, 1986). Figure 1 also shows the six locations that were used in the ocean experiments. They were chosen to represent mid-latitude, subtropical, and tropical regions and to represent a variety of distances from the initial sources of smoke.

Since no present-day atmospheric general circulation model simulates the real atmosphere perfectly, it was not surprising to find that the mean wind stress and surface heat fluxes computed in the atmospheric control simulation differed somewhat from climatology. Therefore, to provide more realistic atmospheric forcing to the ocean in the control experiment and presumably also in the nuclear winter experiment, the wind stress and heat fluxes from the atmospheric simulations were calibrated to climatology as follows. The mean surface wind stress τ, downward solar radiation Q_s, long-wave radiation Q_b, and latent (Q_e) and sensible (Q_h) heat fluxes from the atmospheric model control simulation were compared with the corresponding July climatological values of *Esbensen and Kushnir* [1981]. If F denotes one of these quantities (the wind stress or a heat flux component), a calibration constant,

$$C_F = \bar{F}_o/\bar{F}_s \quad (1)$$

was computed for each F at each of the ocean locations shown in Figure 1. In (1), the overbar represents an average over the month of July, and the subscripts "o" and "s" denote observed [*Esbensen and Kushnir*, 1981] and simulated (control experiment), respectively. The resulting values of C_F are shown in Table 1. Many of the values are near unity, indicating that the mean surface fluxes from the July control simulation agree quite well with July climatology. The anomalous value of $C_F = 5$, associated with $F = Q_e$ at point 3, is caused by the occurrence of very small values of Q_e at that location. A cali-

TABLE 1. Surface Forcing Calibration Factors C_F, Computed From (1) as is Described in the Text

Point	Location	Q_s	Q_b	Q_e	Q_h	τ
1	50°N, 150°W	0.54	1.00	1.00	1.00	2.10
2	50°N, 150°E	0.68	1.67	1.50	0.45	0.90
3	50°N, 50°W	0.67	0.83	5.00	0.45	0.42
4	30°N, 150°W	0.72	1.06	1.62	1.00	2.08
5	10°N, 150°W	0.96	0.95	0.73	0.38	1.02
6	30°N, 125°E	0.75	0.49	0.59	1.00	0.84

TABLE 2. Thirty-Day Mean of the Calibrated Surface Heat Fluxes in Watts per Square Meter and Wind Stresses (10^{-1} N m^{-2}) Used to Drive the Ocean Model in the Control (C) and Nuclear Winter (NW) Experiments

		Q_s		Q_b		Q_e		Q_h		Q_n		τ	
Point	Location	C	NW	C	NW	C	NW	C	NW	C	NW	C	NW
1	50°N, 150°W	115	87	−26	−36	−13	−25	7	2	83	28	0.76	2.14
2	50°N, 150°E	140	63	−35	−55	−15	−49	5	−3	95	−44	0.45	0.90
3	50°N, 50°W	179	78	−35	−24	−16	−50	10	8	138	12	0.45	0.36
4	30°N, 150°W	209	143	−65	−36	−120	−105	−6	−4	18	−2	0.75	1.69
5	10°N, 150°W	190	140	−55	−38	−130	−128	−5	−12	0	−36	1.30	1.25
6	30°N, 125°E	210	119	−35	−27	−59	−199	6	−113	122	−220	0.75	1.44

The heat flux components Q_s, Q_b, Q_e, and Q_h are defined in the text, and $Q_n = Q_s - (Q_b + Q_e + Q_h)$ is the net heat flux. Positive values indicate a downward flux of heat into the ocean.

brated time series of the surface fluxes at each location was constructed by multiplying the 6-hourly values of τ, Q_s, Q_b, Q_e, and Q_h, produced by the atmospheric model simulations, by the appropriate calibration constant in Table 1. Note that as a consequence, both the mean and the standard deviation of the fluxes are modified by the same factor, C_F. This procedure guarantees that the time series of each component of the surface forcing that drives the ocean model in the control experiment has as its mean the corresponding observed climatological mean for July. This constraint on the mean of the atmospheric forcing terms is needed to assure a realistic control state in the ocean. By using the same calibration factors in both the control and the nuclear winter experiment, we essentially assume that the biases in the atmospheric model fluxes are unaffected by nuclear winter.

Table 2 shows a summary of the calibrated surface fluxes that were used in the ocean experiments. It can be seen that the atmospheric nuclear winter experiment produced significant changes in the surface wind stress and heat fluxes at most of the geographical locations studied. More specifically, the average wind stress increased (almost doubled) at four locations, while the net heat flux decreased at all six locations. The largest decrease in net heat flux occurred at the three ocean locations (points 2, 3, and 6) lying directly downwind of the smoke sources. On the other hand, much smaller decreases occurred in the eastern North Pacific Ocean (points 1, 4, and 5). These decreases in the net surface heat flux were largely due to decreased solar radiation caused by the direct absorption of solar radiation by the smoke. However, at point 6, which is located in the East China Sea, the decreased net heat flux is primarily due to a very large, and to some extent unrealistic (see below), increase in the surface evaporation.

At each location, the ocean model was driven by the calibrated values of the surface fluxes computed every 6 hours from the atmospheric simulations. The precipitation rate from the simulations was also used to compute the surface salinity flux needed by the ocean model. However, for brevity and because the response of the salinity in the nuclear winter experiments was generally small, neither precipitation nor salinity will be discussed in this note.

The initial conditions for the ocean experiments consisted of temperature and salinity profiles from the surface to a depth of 200 m. The same initial conditions were used in both the control experiment and the nuclear winter experiment. The initial conditions were based on climatological profiles of temperature and salinity for July at each location, obtained from Fleet Numerical Oceanography Center (FNOC) in Monterey, California). Model sensitivity tests indicate that the response of the upper ocean in these experiments is not sensitive to the particular initial conditions used as long as they are reasonably representative of July conditions at the location in question.

OCEAN RESULTS

The response of the sea surface temperature (SST) and mixed layer depth (MLD) in the control and nuclear winter experiments is shown in Figures 2 and 3. Looking first at the SST (Figure 2), we see that at each location studied the temperature is lower at the end of the nuclear winter experiment than it is at the end of the control experiment. The drop in SST due to the nuclear exchange is typically 3°–5°C, although it is less than 1°C at two locations and more than 8°C at another. Where a significant difference develops between the control and nuclear winter SSTs, the difference develops quite suddenly, usually over a period of only a few days. At two such locations (50°N, 150°W and 50°N, 150°E), the difference develops because of a sudden anomalous cooling of the upper ocean which takes place during the nuclear winter experiment, while at two other locations the difference develops because a short period of strong warming which occurs in the control experiment does not occur in the nuclear winter experiment. This difference between the control and nuclear winter SSTs begins to develop at a different time at each location, depending on the distance upwind to the nearest source of smoke. In mid-latitudes, where many of the experimental points are located, the smoke is transported generally eastward. Thus the smoke-induced cooling begins after only 3 days in the western North Atlantic off the coast of Newfoundland (50°N, 50°W), but it does not start until about day 12–15 in the eastern North Pacific (50°N, 150°W). The locations farther south in the North Pacific (30°N, 150°W and 10°N, 150°W) are not only far downwind but also far to the south of the smoke source. As a result, the response of the upper ocean to the smoke injection is very small at these locations.

At most of the locations shown in Figure 2, the differences between the control and nuclear winter SST's become relatively constant in time after about 2 or 3 weeks. An important exception to this behavior occurs at the point located in the East China Sea (30°N, 125°E), where the SST in the nuclear winter experiment is still falling in relation to the control experiment after 30 days. As was noted above in connection with the surface fluxes (Table 2), the nuclear exchange has a rather unique effect on the surface heat fluxes at this location. Here, in the atmospheric nuclear winter simulation, the atmosphere extracts extremely large amounts of sensible and latent heat from the underlying ocean. We can see from Table 2 that the

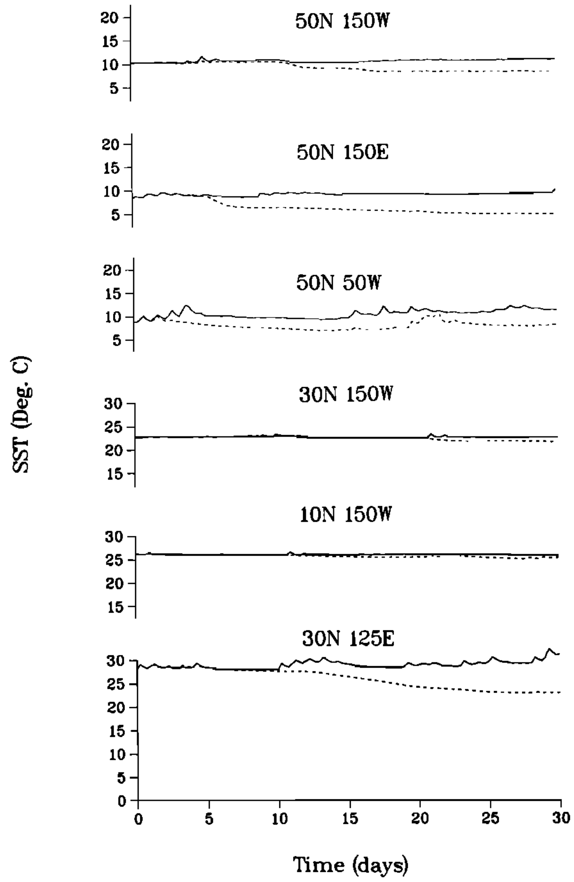

Fig. 2. Time evolution of the SST at each ocean location in the control (solid line) and nuclear winter (dashed) experiment.

increased sensible plus latent heat flux at this location accounts for 259 W m^{-2} of the 342 W m^{-2} decrease in the net surface heat flux which takes place during the nuclear winter experiment. Such extreme surface fluxes, which do not occur at any of the other locations studied, are caused in part by strong winds (see τ values in Table 2) and very cold, dry air which develops upstream over the nearby Asian continent during the atmospheric nuclear winter simulation. Another reason for the large heat loss at the surface is the fact that the SSTs are quite high in the East China Sea in July, and these high SSTs are held constant throughout the atmospheric nuclear winter simulation. Because of this, the sensible and latent heat fluxes at this location and our ocean model's predicted large response may be somewhat unrealistic. In a synchronously coupled atmosphere-ocean model simulation of nuclear winter, in which the SSTs are allowed to change in response to the computed surface fluxes, these fluxes would certainly tend to decrease as the SST decreases. Such decreased fluxes would act to reduce the SST changes, but they could also alter the subsequent atmospheric circulation. It is therefore not possible, using our present results, to estimate with any certainty what the ocean's response in such a coupled nuclear winter experiment would be. In the absence of additional information or further model tests, we feel it is safe to assume that the predicted response of the SST at 30°N, 125°E in Figure 2 represents an upper bound for the change that might actually occur at that location during a nuclear winter. Knowing the upper bound on the ocean's response, and knowing some of the ocean processes that are involved, is an important first step toward the ultimate goal of determining the true response of the coupled ocean-atmosphere system.

Turning now to the MLD (Figure 3), we see that at a majority of the locations studied, the MLD generally becomes deeper during the nuclear winter experiment than during the control experiment. As shown here, the MLD refers to the turbulent boundary layer depth, a prognostic variable in the ocean model. Being the instantaneous depth of penetration of turbulent mixing in the upper ocean, the MLD will not necessarily correspond to the conventional definition of mixed layer depth, namely, the depth at which the temperature drops to the value 0.2°C below the SST, although there is a strong similarity between the two. The distinction is especially relevant during those periods, usually of short duration, when the MLD has shallowed. In these cases, the temperature drop below the MLD can be very small. Nevertheless, at the three high-latitude points studied (i.e., at 50°N), a noticible deepening of the oceanic boundary layer occurs in the nuclear winter experiment at the time when the corresponding SST (Figure 2) first begins to differ from the control SST. Off Newfoundland (50°N, 50°W), however, the MLD slowly recovers from its sudden response to nuclear winter, and by the end of the experiment it is very similar to that in the control experiment. At the East China Sea location, the MLD in the nuclear winter experiment does not shallow on day 10 as it does in the control experiment, and this is when the two SSTs (control and nuclear winter (Figure 2)) suddenly begin to depart from each other.

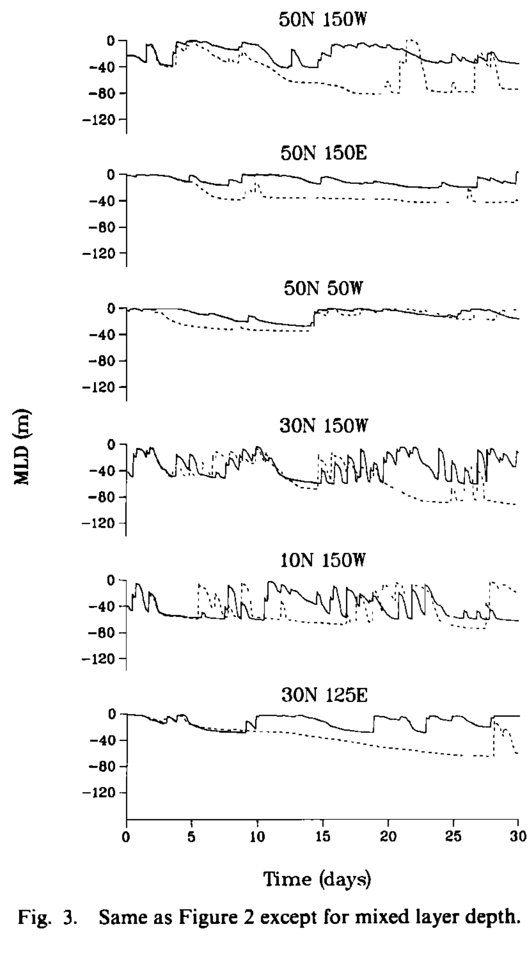

Fig. 3. Same as Figure 2 except for mixed layer depth.

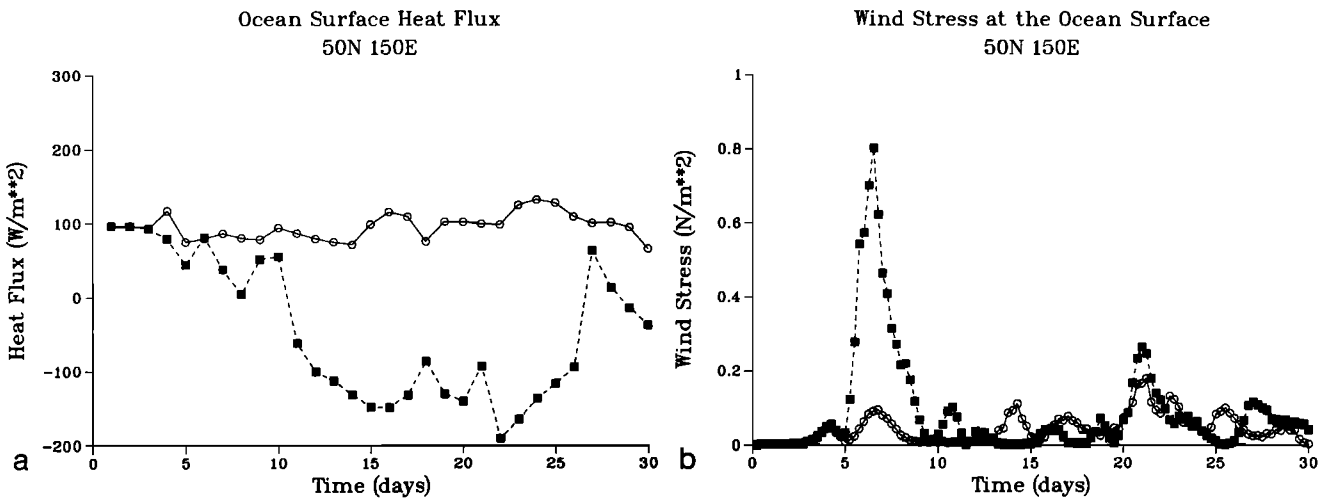

Fig. 4. Time evolution of the calibrated (*a*) net surface heat flux Q_n and (*b*) surface wind stress τ at 50°N, 150°E used in the control experiment (solid lines) and the nuclear winter experiment (dashed).

By examining Table 2 and Figures 2 and 3, it is possible to determine for each geographical location whether the model-simulated SST decrease during the nuclear winter experiment was due to enhanced air-sea cooling or entrainment. For example, at the first location (50°N, 150°W), the net heat flux into the ocean was 55 W m^{-2} less during the nuclear winter experiment than during the control experiment (Table 2). If the average MLD at this location during nuclear winter is taken to be 50 m (Figure 3), this decrease in surface heat flux cannot account for more than a 1°C difference in SST at the end of the month. This implies that well over half of the 2.8°C decrease in SST in the nuclear winter experiment (Figure 2) was caused by entrainment. This interpretation is also consistent with the much greater wind stress, an important factor in producing entrainment, experienced during nuclear winter at this location (Table 2). In the same way, we find that more than half of the decrease in SST at the second geographical location (50°N, 150°E) is due to a decrease in the net surface heat flux, with the rest due to enhanced entrainment (see Figure 5*b*, and additional discussion below). At the third location (50°N, 50°W), where there was little change in the wind stress and MLD due to nuclear winter, all of the SST decrease is attributed to the rather large decrease (126 W m^{-2}) in the net surface heat flux. The only other location where the SST response was significant is the East China Sea point (30°N, 125°E), and there most of the SST decrease is accounted for simply by the very large change in the net surface heat flux caused by the extraordinary sensible and latent heat fluxes noted above.

We now examine the response of the upper ocean to nuclear winter in greater detail by describing the time evolution of the vertical thermal structure and its relation to the atmospheric forcing at one of the experimental ocean locations. The point at 50°N, 150°E is chosen for this purpose because the atmospheric forcing during the control and nuclear winter experiments at this location is fairly representative of the other locations as well. This point, located approximately 500 km west of the southern tip of the Kamchatka peninsula in the sea of Okhotsk, experiences a doubling of the average wind stress and a 139 W m^{-2} decrease in the net surface heat flux due to the smoke injection (Table 2). The results for this point are shown in Figures 4 and 5.

Looking first at the atmospheric forcing (Figure 4), we see that the net heat flux is affected by the smoke as early as July 3, and that an exceptionally strong wind event lasting several days occurs shortly thereafter. For 16 consecutive days during the nuclear winter experiment, from July 11 to 26, the solar radiation is reduced essentially to zero by the thick smoke cloud originating over nearby Siberia, and this produces a net heat loss ($Q_n < 0$) which lasts almost to the end of the month. By the end of the month, the net heat flux has partially returned to normal. Except for the enormous wind storm during the first week, the wind stress is quite similar in the two experiments. This characteristic of a strong wind event early in the month, followed by severe reductions in solar radiation and subsequent partial recovery, is typical of the atmospheric forcing during nuclear winter at other locations as well.

The response of the upper ocean thermal structure (Figure 5) is easily understood in terms of the above forcing. During the control experiment, the upper ocean responds to a cycle of typical summer wind events on July 6, 13, 16, 21, and 25. The ocean's response to these wind events is seen in the deepening and coalescense of the isotherms representing an enhanced vertical temperature gradient at the base of the mixed layer caused by the wind-generated downward mixing of warm surface layer water. In between these characteristically gentle wind events, the isotherms tend to spread out in the vertical as the mixed layer shallows and warms owing to the net surface heating. The evolution during the nuclear winter experiment is very different. The wind storm on July 5 deepens and cools the mixed layer, and the subsequent negative (upward) heat flux and relatively normal winds produce a gradual cooling and slow deepening of the mixed layer during the remainder of the month. In spite of the drastic changes in the atmospheric forcing during the nuclear winter experiment, the response of the ocean is confined to the upper 60 m.

Discussion

In this study we have examined the short-term response of the upper ocean to the simulated forcing of a hypothetical atmospheric nuclear winter. The atmospheric forcing was derived from fields produced by a two-level atmospheric general circulation model in both a control and a nuclear winter simulation. The ocean was represented by a one-dimensional

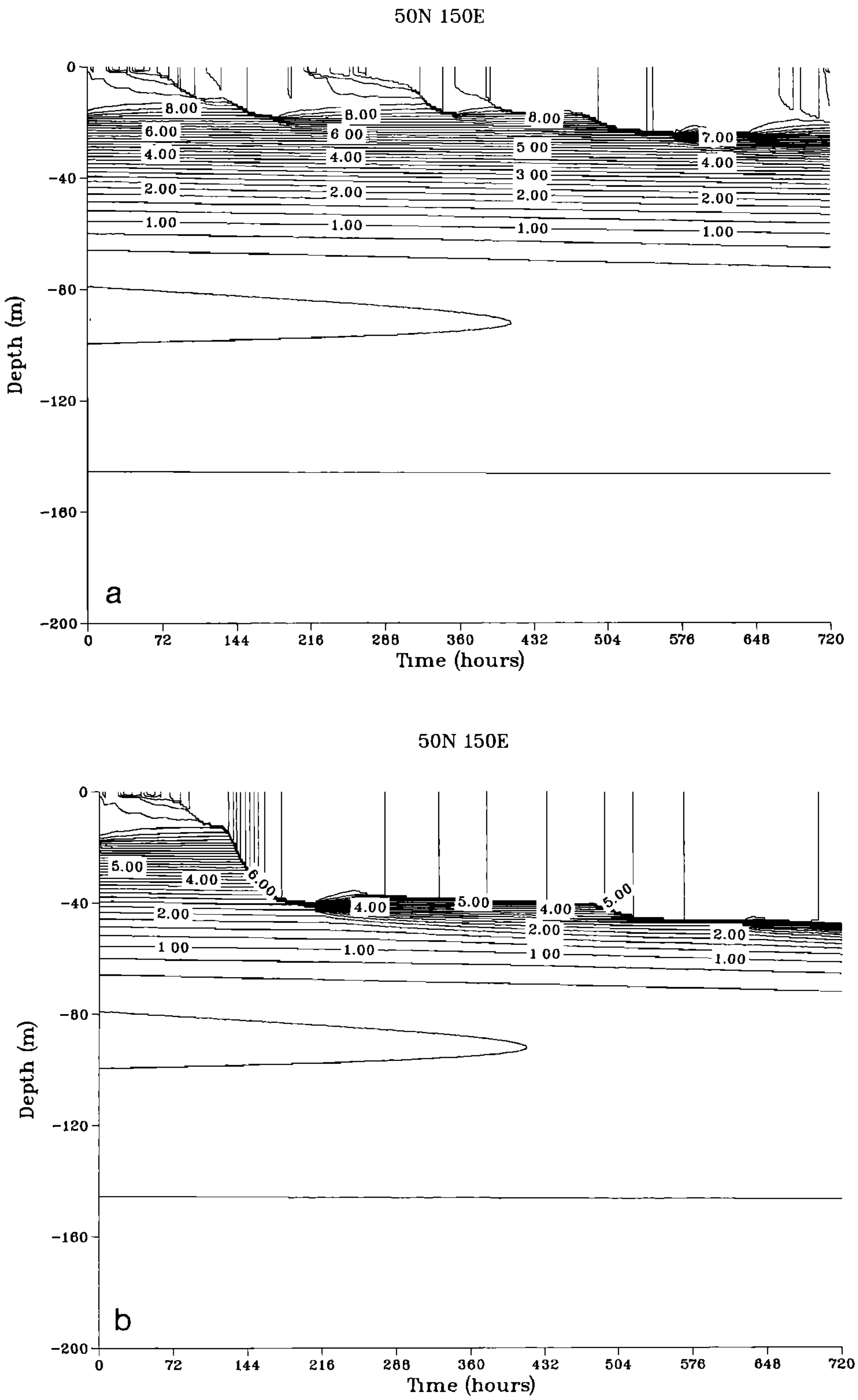

Fig. 5. Temperature (in degrees Celsius) as a function of time (0–30 days) and depth (0–200 m) at 50°N, 150°E in the (*a*) control and (*b*) nuclear winter experiments.

mixed layer model applied at six different locations in the North Atlantic and North Pacific oceans. Since there was no negative feedback with regard to the heat exchange between the ocean and atmosphere, the intensity of the modeled ocean response may be regarded as an upper bound (i.e., the actual response may be weaker). This is a useful thing to know, particularly for estimating the size of the feedback from the ocean and its potential effect on the atmosphere.

Our results indicate that at some of the locations, depending on the distance upwind from the point in question to the nearest source of smoke, the upper ocean experiences a significant cooling in response to a large scale nuclear exchange.

TABLE 3. Difference Between the Model Simulated SST at the End of the Two Experiments (Control Minus Nuclear Winter = ΔT_{smoke}) and the Observed Change in SST During a Climatological Seasonal Cycle (Summer Minus Winter = $\Delta T_{seasonal}$)

Point	Location	ΔT_{smoke}	$\Delta T_{seasonal}$
1	50°N, 150°W	2.8	9.0
2	50°N, 150°E	5.0	8.0
3	50°N, 50°W	3.5	4.0
4	30°N, 150°W	1.0	5.0
5	10°N, 150°W	0.5	2.0
6	30°N, 125°E	8.5	12.0

All temperature differences are in degrees Celsius, with climatological values from *Robinson* [1976] for the North Pacific Ocean (points 1, 2, 4, 5, and 6) and from *Reynolds* [1982] for the North Atlantic Ocean (point 3).

This cooling produces a decrease in the SST which can be a sizeable fraction of the normal seasonal cycle at the location in question (Table 3). Thus in the eastern North Pacific Ocean along 150°W the decrease in SST due to the nuclear exchange is approximately 30% of the normal seasonal change. At the other three locations, which happen to lie closer and downwind of the source of smoke in the atmosphere (Figure 1), the decrease in SST due to the nuclear exchange is about 75% of the normal seasonal change. With the exception of the East China Sea location discussed earlier, this cooling is caused primarily by the smoke induced decrease in solar radiation. Additional cooling is produced by enhanced sensible plus latent heat flux and entrainment, but the combined effect of these processes is generally smaller than the effect of decreased solar radiation (Table 2). The East China Sea location is unique because of the extremely large increase in the sensible plus latent heat flux that occurred at that location during the nuclear winter experiment. As was discussed above, this very large heat loss to the atmosphere at the surface is considered to be somewhat unrealistic because the ocean surface temperatures were kept at their July climatological values throughout the atmospheric nuclear winter simulation. A more realistic, coupled ocean-atmosphere model would most likely produce smaller air-sea fluxes and thereby result in a weaker ocean response in this region. Nevertheless, the relatively large ocean response at the East China Sea location tentatively suggests that locations such as this, having rather high SSTs initially and lying immediately downwind of a large land mass experiencing a nuclear winter, are likely to experience the largest SST decreases in response to a nuclear exchange.

We have presented results for only six selected geographical points, an admittedly small sample. Whether or not our results are representative of other oceanic regions can be estimated to some extent by examining the geographical distribution of the smoke-induced changes in the mean wind stress and surface heating, as is simulated by the general circulation model (Figure 6). Such an examination indicates that both increased wind stress and decreased surface heating are quite typical of the response to the smoke for the northern hemisphere oceans; regions of reduced wind stress or enhanced surface heating are generally confined to land surfaces and/or the southern hemisphere. Regions of particularly intense surface cooling are found in the Sea of Japan and in the Bay of Bengal, associated with enhanced convective fluxes as cold continental air drains from the Tibetan plateau. Broad bands of enhanced wind stress are found in the western Pacific, far eastern Pacific, and western Atlantic oceans at 10°N latitude. They reflect a westerly acceleration of the zonal flow by the enhanced Hadley circulation driven by a smoke-induced meridional heating gradient [*Covey et al.*, 1984].

At the present time it is very difficult to evaluate the significance of the ocean's short-term response to the kind of large-scale nuclear exchange postulated in this work, and it is virtually impossible to estimate from the present results what the ocean's longer-term response might be. As was noted earlier, a large fraction of the SST change following such a nuclear exchange takes place during a very short period of time, typically just several days (Figure 2). This is quite different from the normal seasonal decrease in SST from summer to winter which occurs over a period of at least several months. Thus there is some indication that 1 month after the smoke is introduced into the atmosphere the SSTs are approximately following the normal annual cycle (i.e., that of the control experiment) only at a lower value of the temperature. However, our experiments are too short, and the modeling and experimental uncertainties are too great, to allow us to infer anything about

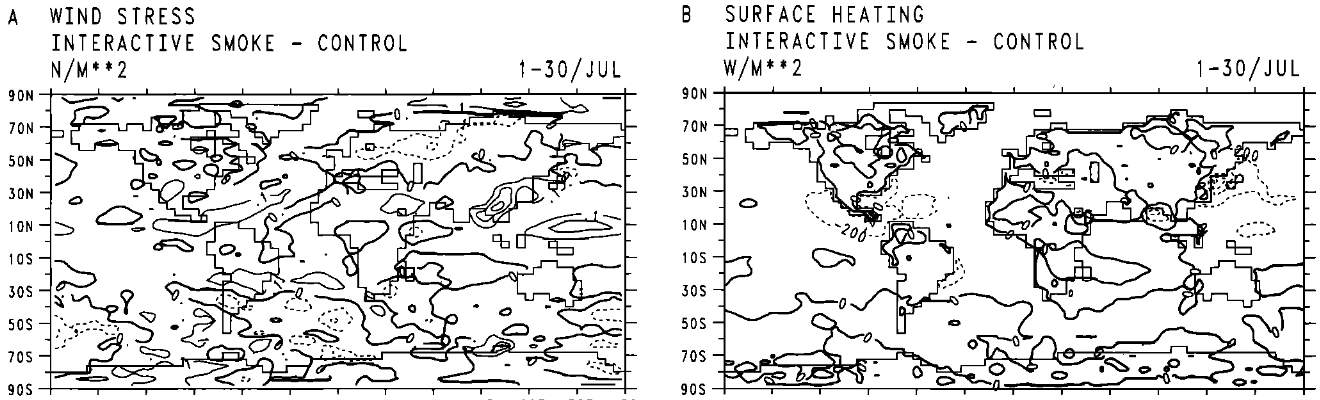

Fig. 6. Global distribution of the change in the 30-day mean surface (*a*) wind stress and (*b*) heat flux from the control experiment to the nuclear winter experiment. The wind stress is in units of newtons per square meter with a contour interval of 0.1, and the heat flux is in units of watts per square meter with a contour interval of 200. Dashed contours indicate negative values.

changes that might occur in the ocean on, say, the seasonal time scale. Indeed, some of our results, e.g., those at the East China Sea location, suggest that it may be necessary in the future to use a coupled ocean-atmosphere model to properly address such important questions.

Acknowledgments. We wish to thank Penelope Jones for her diligent typing of the manuscript, which evolved through several drafts. Computer time for the ocean experiments was provided by the W. R. Church Computer Center at the Naval Postgraduate School. This research (by RLH and RWG) was supported by the Office of Naval Research (code 1122P0) under contract N0001486AF00001. The work of SJG was performed under the auspices of the U. S. Department of Energy by the Lawrence Livermore National Laboratory under contract W-7405-Eng-48. This support is gratefully acknowledged.

REFERENCES

Aleksandrov, V. V., and G. L. Stenchikov, Numerical simulation of the climatic consequences of a nuclear war, *USSR Comput. Math. Math. Phys.*, *24*, 87–90, 1984.

Berger, A., Nuclear winter or nuclear fall?, *Eos Trans. AGU*, *67*, 617–621, 1986.

Cess, R. D., G. L. Potter, S. J. Ghan, and W. L. Gates, The climatic effects of large injections of atmospheric smoke and dust: A study of climatic mechanisms with one- and three-dimensional climate models. *J. Geophys. Res.*, *90*, 12,937–12,950, 1985.

Covey, C., S. H. Schneider, and S. L. Thompson, Global atmospheric effects of massive smoke injections from a nuclear war: Results from general circulation model simulations, *Nature*, *308*, 21–25, 1984.

Crutzen, P. J., and J. W. Birks, The atmosphere after a nuclear war: Twilight at noon, *Ambio*, *11*, 115–125, 1982.

Esbensen, S. K., and Y. Kushnir, The heat budget of the global ocean: An atlas based on estimates from surface marine observations, *Rep. 29*, 27 pp., Clim. Res. Inst., Oreg. State Univ., Corvallis, 1981.

Garwood, R. W., Jr., An oceanic mixed layer model capable of simulating cyclic states, *J. Phys. Oceanogr.*, *7*, 455–468, 1977.

Ghan, S. J., J. W. Lingaas, M. E. Schlesinger, R. L. Mobley, and W. L. Gates, A documentation of the OSU two-level atmospheric general circulation model, *Rep. 35*, 395 pp., Clim. Res. Inst., Oreg. State Univ., Corvallis, 1982.

Ghan, S. J., M. C. MacCracken, and J. J. Walton, Climatic response to large summertime injections of smoke in the atmosphere: Changes in precipitation and the Hadley circulation, *Rep. VCRL-92324*, Lawrence Livermore Natl. Lab., Livermore, Calif., 1985.

Haberle, R. M., T. P. Ackerman, O. B. Toon, and J. L. Hollingsworth, Global transport of atmospheric smoke following a major nuclear exchange, *Geophys. Res. Lett.*, *12*, 405–408, 1985.

MacCracken, M. C., Nuclear war: Preliminary estimates of the climatic effects of a nuclear exchange, *Rep. UCRL-89770*, Lawrence Livermore Natl. Lab., Livermore, Calif., 1983.

MacCracken, M. C., and J. J. Walton, The effects of interactive transport and scavenging on the calculated temperature change resulting from large amounts of smoke, *Rep. UCRL-91446*, Lawrence Livermore Natl. Lab., Livermore, Calif., 1984.

Malone, R. C., L. H. Auer, G. A. Glatzmaier, M. C. Wood, and O. B. Toon, Nuclear winter: Three-dimensional simulations including interactive transport, scavenging, and solar heating of smoke, *J. Geophys. Res.*, *91*, 1039–1053, 1986.

Martin, P. J., Simulation of the mixed layer at OWS November and Papa with several models, *J. Geophys. Res.*, *90*, 903–916, 1985.

Reynolds, R. W., A monthly averaged climatology of sea surface temperature, *Tech. Report NWS31*, Natl. Weather Serv., Natl. Oceanic and Atmos. Admin., Rockville, Md., 1982.

Robinson, M. K., Atlas of North Pacific Ocean monthly mean temperatures and mean salinities of the surface layer, *Rep. NOORP-2*, 192 pp., Naval Oceanogr. Office, Washington, D. C., 1976.

Robock, A., Snow and ice feedbacks prolong effects of nuclear war, *Nature*, *310*, 667–670, 1984.

Schlesinger, M. E., and W. L. Gates, The January and July performance of the OSU two-level atmospheric general circulation model, *J. Atmos. Sci.*, *37*, 1914–1943, 1980.

Sellers, W. D., A new global climate model, *J. Appl. Meteorol.*, *12*, 241–254, 1973.

Stenchikov, G., Climatic consequences of nuclear war, in *The Night After*, 165 pp., Mir, Moscow, 1985.

Thompson, S. L., Global interactive transport simulations of nuclear war smoke, *Nature*, *311*, 35–39, 1985.

Turco, R. P., O. B. Toon, T. P. Ackerman, J. B. Pollack, and C. Sagan, Nuclear winter: Global consequences of multiple nuclear explosions, *Science*, *222*, 1283–1292, 1983.

R. W. Garwood, Jr., Department of Oceanography, Naval Postgraduate School, Monterey, CA 93943.

S. J. Ghan, Lawrence Livermore National Laboratory, University of California, Livermore, CA, 94550.

R. L. Haney and T. R. Mettlach, Department of Meteorology, Naval Postgraduate School, Monterey, CA 93943.

(Received March 12, 1986;
accepted October 13, 1986.)